Transmission of one predicts another: Apathogenic proxies for transmission dynamics of a fatal virus

Marie L.J. Gilbertson[1†], Nicholas M. Fountain-Jones[2*], Jennifer L. Malmberg[3,4*], Roderick B. Gagne[3,5], Justin S. Lee[3], Simona Kraberger[6], Sarah Kechejian[3], Raegan Petch[3], Elliott Chiu[3], Dave Onorato[7], Mark W. Cunningham[8], Kevin R. Crooks[9], W. Chris Funk[10], Scott Carver[2], Sue VandeWoude[3], Kimberly VanderWaal[1], Meggan E. Craft[1,11]

[†]Corresponding author: jone1354@umn.edu

*These authors contributed equally

[1]Department of Veterinary Population Medicine, University of Minnesota, St Paul, MN 55108.

[2]School of Natural Sciences, University of Tasmania, Hobart Australia 7001.

[3]Department of Microbiology, Immunology, and Pathology, Colorado State University, Fort Collins, CO 80523

[4]Department of Veterinary Sciences, University of Wyoming, Laramie, Wyoming 82071.

[5]Wildlife Futures Program, Department of Pathobiology, University of Pennsylvania School of Veterinary Medicine, Philadelphia, PA 19104

[6]The Biodesign Center for Fundamental and Applied Microbiomics, Arizona State University, Tempe, Arizona, AZ 85287, USA

[7]Fish and Wildlife Research Institute, Florida Fish and Wildlife Conservation Commission, Naples, FL 34114.

[8]Fish and Wildlife Research Institute, Florida Fish and Wildlife Conservation Commission, Gainesville, FL 32601.

[9]Department of Fish, Wildlife, and Conservation Biology, Colorado State University, Fort Collins, CO 80523.

[10]Department of Biology, Graduate Degree Program in Ecology, Colorado State University, Fort Collins, CO 80523.

[11] Department of Ecology, Evolution and Behavior, University of Minnesota, St Paul, MN 55108.

Abstract

Identifying drivers of transmission prior to an epidemic—especially of an emerging pathogen—is a formidable challenge for proactive disease management efforts. We tested a novel approach in the Florida panther, hypothesizing that apathogenic feline immunodeficiency virus (FIV) transmission could predict transmission dynamics for pathogenic feline leukemia virus (FeLV). We derived a transmission network using FIV whole genome sequences, and used exponential random graph models to determine drivers structuring this network. We used these drivers to predict FeLV transmission pathways among panthers and compared predicted outbreak dynamics against empirical FeLV outbreak data. FIV transmission was primarily driven by panther age class and distances between panther home range centroids. Prospective FIV-based modeling predicted FeLV dynamics at least as well as simpler, often retrospective approaches, with evidence that FIV-based predictions captured the spatial structuring of the observed FeLV outbreak. Our finding that an apathogenic agent can predict transmission of an analogously transmitted pathogen is an innovative approach that warrants testing in other host-pathogen systems to determine generalizability. Use of such apathogenic agents holds promise for improving predictions of pathogen transmission in novel host populations, and could thereby provide new strategies for proactive pathogen management in human and animal systems.

Keywords

transmission tree; exponential random graph model; network modeling; disease model; Florida panther; transmission heterogeneity

Introduction

Infectious disease outbreaks can have profound impacts on conservation, food security, and global health and economics. Mathematical models have proven a vital tool for understanding transmission dynamics of pathogens [1], but struggle to predict the dynamics of novel or emerging agents [2]. This is at least partially due to the challenges associated with characterizing contacts relevant to transmission processes. Common modeling approaches that assume all hosts interact and transmit infections to the same degree ignore key drivers of transmission. Such drivers can include specific transmission-relevant behaviors including grooming or fighting in animals [3], concurrent sexual partnerships in humans [4], or homophily [5], and result in flawed epidemic predictions [6,7]. Further, identifying drivers of transmission and consequent control strategies for any given pathogen is typically done reactively or retrospectively in an effort to stop or prevent further outbreaks or spatial spread (e.g. [8,9]). These constraints limit the ability to perform prospective disease management planning tailored to a given target population, increasing the risk of potentially catastrophic pathogen outbreaks, as observed in humans [10], domestic animals [11], and species of conservation concern (e.g., [12–14]).

A handful of studies have evaluated whether common infectious agents present in the healthy animal microbiome or virome can indicate contacts between individuals that may translate to interactions promoting pathogen transmission [15–22]. Such an approach circumvents some of the uncertainties associated with more traditional approaches to contact detection [6]. In these cases, genetic evidence from the transmissible agent itself is used to define between-individual interactions for which contact was sufficient for transmission to occur. Results of such studies show mixed success [15–18]. For example, members of the same household [19,20] or animals with close social interactions [21,22] have been found to share microbiota, but disentangling social mechanisms of this sharing is complicated by shared diets, environments, and behaviors [23].

79 These studies have, however, revealed ideal characteristics of non-disease inducing
80 infectious agents (hereafter, *apathogenic agents*) for use as markers of transmission-relevant
81 interactions. Such apathogenic agents should have rapid mutation rates to facilitate discernment
82 of transmission relationships between individuals over time [24,25]. Furthermore, these agents
83 should be relatively common and well-sampled in a target population, have a well-characterized
84 mode of transmission that is similar to the pathogen of interest, and feature high strain alpha-
85 diversity (local diversity) and high strain turnover [25,26]. RNA viruses align well with these
86 characteristics [27] such that apathogenic RNA viruses could act as "proxies" of specific modes
87 of transmission (i.e., direct transmission) and indicate which drivers underlie transmission
88 processes. Such drivers, including but not limited to host demographics, relatedness, specific
89 behaviors, or space use, would subsequently allow prediction of transmission dynamics of
90 pathogenic agents with the same mode of transmission [25].
91 Here, we test the feasibility of this approach using a naturally occurring host-pathogen
92 system to test if an apathogenic RNA virus can act as a proxy for direct transmission processes
93 and subsequently predict transmission of a pathogenic RNA virus. Florida panthers (*Puma*
94 *concolor coryi*) are an endangered subspecies of puma found only in southern Florida. We have
95 documented that this population is infected by several feline retroviruses relevant to our study
96 questions [28,29]. Feline immunodeficiency virus (FIVpco; hereafter, FIV) occurs in
97 approximately 50% of the population and does not appear to cause significant clinical disease
98 [28]. FIV is transmitted by close contact (i.e., fighting and biting), generally has a rapid mutation
99 rate (intra-individual evolution rate of 0.00129 substitutions/site/year; [30]), and, as a chronic
100 retroviral infection, can be persistently detected after the time of infection. Panthers are infected
101 with feline leukemia virus (FeLV), also a retrovirus, which caused a well documented, high
102 mortality outbreak among panthers in 2002-2004 [29]. FeLV infrequently spills over into
103 panthers following exposure to infected domestic cats [31]. Once spillover occurs, FeLV is
104 transmitted between panthers by close contact and results in one of three infection states:

progressive, regressive, or abortive infection [29]. Progressive cases are infectious and result in mortality; regressive infections are unlikely to be infectious—though this is unclear in panthers—and recover [29,32,33]. Abortive cases clear infection and are not themselves infectious [32].

The objectives of this study were therefore: (1) to determine which drivers shape FIV transmission in Florida panthers, and (2) test if these drivers can predict transmission dynamics of analogously transmitted FeLV in panthers. Success of this approach in our model system would pave the way for testing similar apathogenic agents in other host-pathogen systems, thereby improving our understanding of drivers of individual-level heterogeneity in transmission, and consequently our ability to predict transmission dynamics of novel agents in human and animal populations.

Methods

Dataset assembly

We assembled an extensive dataset covering almost 40 years of Florida panther research and including panther sex and age class. A subset of the population is monitored using very high frequency (VHF) telemetry collars, with relocations determined via aircraft typically three times per week. Previous panther research has generated a microsatellite dataset for monitored panthers [34], and a dataset of 60 full FIV genomes (proviral DNA sequenced within a tiled amplicon framework in [35]). In addition, to augment observations from the 2002-04 FeLV outbreak [29], we leveraged an FeLV database which documents FeLV status (positive and negative) for 31 panthers from 2002-04 as determined by qPCR.

FIV transmission inference

To determine drivers of FIV transmission, we first generated a “who transmitted to whom” transmission network using 60 panther FIV genomes collected from 1988 to 2011 (average of minimum annual panther counts across this period was 62.3 panthers; [36]). We

131 used the program Phyloscanner [37] (see Figure 1 for workflow across all analyses), which
132 assumes both within- and between-host evolution when inferring transmission relationships
133 between sampled and even unsampled hosts [37]. Phyloscanner operates in a two step
134 process, first inferring within- and between-host phylogenies in windows along the FIV genome.
135 Then, using the within-host viral diversity gleaned from deep sequencing, Phyloscanner
136 functionally performs ancestral state reconstruction to infer transmission relationships between
137 hosts, outputting transmission trees or networks. For Phyloscanner's step one, we used 150bp
138 windows, allowing 25bp overlap between windows. To test sensitivity to this choice, we
139 separately ran a full Phyloscanner analysis with 150bp windows, but without overlap between
140 windows (supplementary methods). The tiled amplicon PCR approach used to generate our FIV
141 genomic data biases for detection of one known variant, such that we did not expect detectable
142 superinfections. In the second step of Phyloscanner, we therefore held the parameter which
143 penalizes within-host diversity (k) equal to 0. We used a patristic distance threshold of 0.05 and
144 allowed missing and more complex transmission relationships. Because we had uneven read
145 depth across FIV genomes, we downsampled to a maximum of 200 reads per host. The output
146 of the full Phyloscanner analysis was a single transmission network (hereafter, *main FIV*
147 *network*), but see supplementary methods for details regarding analysis of the sensitivity of our
148 results to variations in and summary across multiple transmission networks.
149

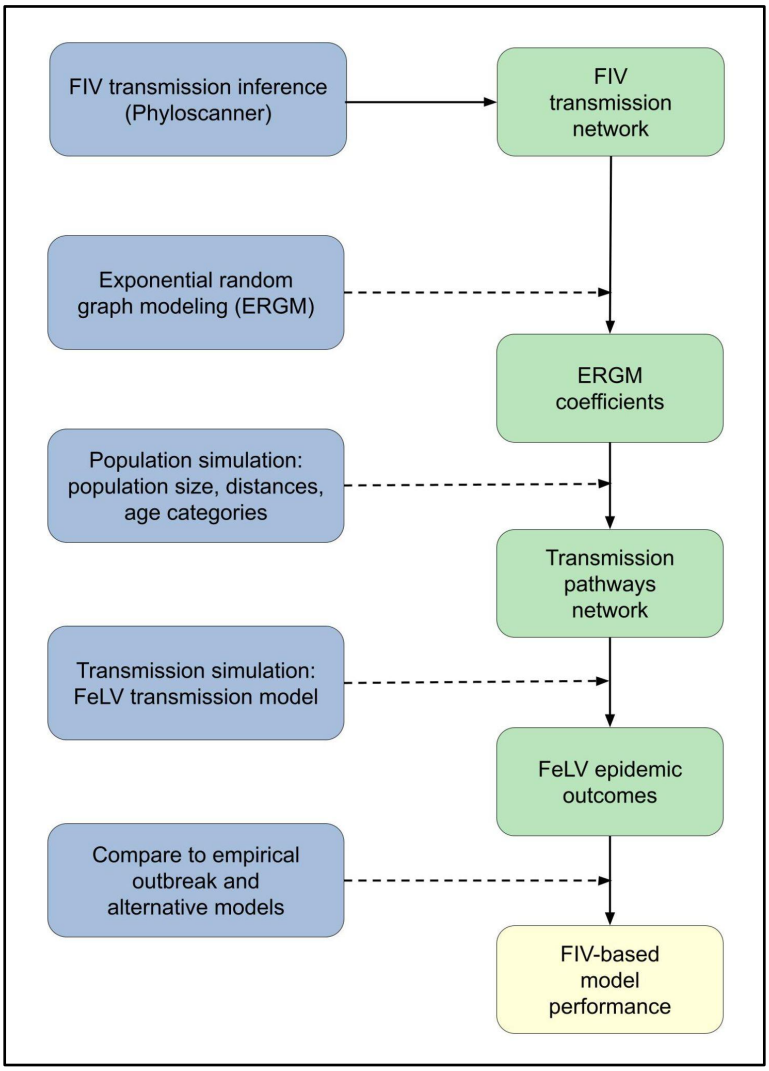

Figure 1: *Conceptual workflow across all analysis steps. Processes are shown on the left in blue; specific outcomes are shown on the right in green; the final analysis outcome is in yellow at the bottom right. Solid lines show direct flows or outcomes. Dashed lines show processes acting on or in concert with prior outcomes: for example, exponential random graph modeling (ERGM) was performed using the FIV transmission network, and the combination of the two produced the ERGM coefficients outcome.*

Statistical analysis of FIV transmission networks

159 Phyloscanner transmission tree output suggests direction of transmission, but in our
160 case, these results were often uncertain (see Results). To avoid putting undue emphasis on an
161 uncertain direction of transmission, we simplified the transmission tree output to undirected,
162 unweighted (binary) networks and performed statistical analysis of these networks using
163 exponential random graph models (ERGMs; [38]). ERGMs model the edges in networks, with
164 explanatory variables representing the potential structural drivers of the observed network [38].
165 By including network structural variables, ERGMs account for the inherent non-independence of
166 network data. As such, we modeled "transmission relationships" (i.e., being connected in the
167 transmission network) as a function of network structural variables and transmission variables
168 we a priori expected to influence direct transmission processes in panthers. We considered
169 several structural variables: an intercept-like edges term [38]; geometrically weighted edgewise
170 shared partner distribution (*gwesp*; representation of network triangles); alternating k-stars
171 (*altkstar*; representation of star structures); and 2-paths (2 step paths from *i* to *k* via *j*; [39]). In
172 addition, we considered a suite of transmission variables (see supplementary methods for
173 additional variable details): panther sex; age class (subadult or adult); pairwise genetic
174 relatedness (panther microsatellite data from [34]); position of panther home range centroid
175 (95% minimum convex polygon) or capture location (hereafter, *centroid*) relative to the major I-
176 75 freeway (locations could be north or south of this east-west freeway); distance from centroid
177 to nearest urban area (in km; USA Urban Areas layer, ArcGIS; [40]); pairwise geographic
178 distance between centroids (log-transformed; Figure S1); and pairwise home range overlap
179 (utilization distribution overlap indices of 95% bivariate normal home range kernels; [41,42]).
180 Because ERGMs are prone to degeneracy with increasing complexity [38], we first
181 performed forward selection for network structural variables, followed by forward selection of
182 dyad-independent variables, while controlling for network structure. Model selection was based
183 on AIC and goodness of fit, and MCMC diagnostics were assessed for the final model
184 (supplementary methods). ERGMs were fit with the *ergm* package [43] in R (v3.6.3; [44]).

185

186 *Panther population simulations*

187 We next simulated FeLV transmission through a network representing panthers during
188 the 2002-04 FeLV outbreak where network edges represented likely transmission pathways
189 based on ERGM-identified predictors of FIV transmission (*FIV-based model*). Hereafter, a *full-*
190 *simulation* includes both simulation of the panther population with its likely transmission
191 pathways and simulation of FeLV transmission within that population. Below, we describe the
192 process for a single simulation, but these procedures were repeated for each full simulation.

193 We first based the simulated population size on the range of empirical estimates from
194 2002-2004 (Table S1; [36]). Additional characteristics of the simulated population included those
195 identified as significant variables in the ERGM analysis: age category and pairwise geographic
196 distances between panther home range centroids (see Results). We randomly assigned age
197 categories to the simulated population based on the proportion of adults versus subadults. Age
198 proportions were based on age distributions in the western United States [45], which
199 qualitatively align with the historically elevated mean age of the Florida panther population [46].
200 Pairwise geographic distances for the simulated population were generated by randomly
201 assigning simulated home range centroids based on the distribution of observed centroids on
202 the landscape (supplementary methods).

203 We then used ERGM coefficients to generate network edges among the simulated
204 panther population using the *ergm* package in R [43]. The FIV transmission network spanned 15
205 years of observations and represents a subset of the actual contact network, as it includes only
206 those interactions that resulted in successful transmission. We therefore had a high degree of
207 uncertainty regarding the appropriate network density for our simulations. To manage this
208 uncertainty, we constrained density (ratio of existing edges to all possible edges) in our network
209 simulations across a range of parameter space (net_dens, Table S1).

210

Simulation of FeLV transmission on FIV-based networks

The next step in each full simulation was to model FeLV transmission through the network generated from FIV predictors of transmission. FeLV transmission was based on a stochastic chain binomial process on the simulated network, following a modified SIR compartmental model (Figure 2). Simulations were initiated with one randomly selected infectious individual and proceeded in weekly time steps. Transmission simulations lasted until no infectious individuals remained or until 2.5 years, whichever came first.

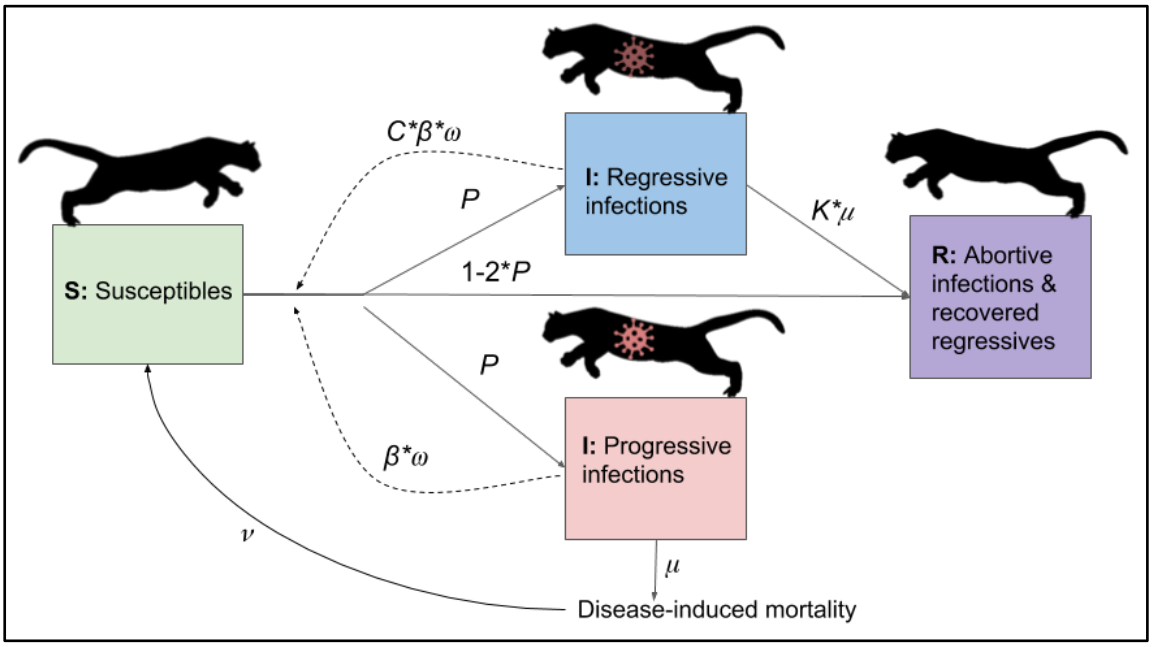

Figure 2: *Diagram of flows of individuals between compartments in transmission model. Virus icons indicate infectious states, with the regressive infection icon darkened to represent reduced or uncertain infectiousness of this class. Note: a vaccination process was also included in the transmission model, but is not shown for simplicity. With vaccination, susceptibles could be vaccinated, and vaccinated individuals subsequently infected as with susceptibles, but with an additional probability of (1-ve). See Table S1 for definitions of parameters.*

227 Transmission was dependent on the following (Figure 2; see Table S1 for parameter
228 definitions): (1) existence of an edge between two individuals, (2) the dyad in question involving
229 a susceptible and infectious individual, and (3) a random binomial draw based on the probability
230 of transmission given contact (β). In addition, *Puma concolor* generally have low expected
231 weekly contact rates [47]; we therefore included a weekly contact probability, represented as a
232 random binomial draw for contact in a given week (ω).
233 Upon successful transmission, infectious individuals were randomly assigned to one of
234 three outcomes of FeLV infection [29]. *Progressive* infections (probability P) are infectious (β),
235 develop clinical disease, and die due to infection (μ). *Regressive* infections (also probability P)
236 recover from infection ($K*\mu$, where K is a constant) and, having entered a state of viral latency,
237 are not considered at risk of FeLV reinfection [29,48]. Using model assumptions derived from
238 known patterns of FeLV infection in domestic cats, regressive individuals are not infectious [29],
239 but given ongoing uncertainty, we included some transmission from regressives ($C*\beta$, where C
240 is a constant). *Abortive* infections (probability 1-2P) are never infectious, clearing infection and
241 joining the recovered class. While the duration of immunity in abortive cases has not been
242 studied in panthers, because abortive cases clear infection through a strong immune response
243 and develop anti-FeLV antibodies, reinfection with FeLV is considered extremely unlikely [48].
244 A vaccination process was included in simulations as panthers were vaccinated against
245 FeLV during the historical FeLV outbreak starting in 2003. Vaccination occurred at a rate, τ, and
246 applied to the whole population, as wildlife managers are unlikely to know if a panther is
247 susceptible at the time of capture or darting. However, only susceptible individuals transitioned
248 to the vaccinated class (i.e. vaccination failed in non-susceptibles). Because panthers were
249 vaccinated in the empirical outbreak with a domestic cat vaccine with unknown efficacy in
250 panthers, we allowed vaccinated individuals to become infected in transmission simulations by
251 including a binomial probability for vaccine failure (1-vaccine efficacy, *ve*, Table S1).

The panther population size remained roughly static through the course of the FeLV outbreak [36]. We therefore elected not to include background mortality, but did include infection-induced mortality. To maintain a consistent population size, we therefore included a birth/recruitment process. Because FIV-based simulated networks drew edges based on population characteristics, we treated births as a “respawning” process, in which territories vacated due to mortality were reoccupied by a new susceptible at rate, ν. This approach allowed us to maintain the ERGM-based network structure and is biologically reasonable, as vacated panther territories are unlikely to remain unoccupied for long.

Comparison of simulation predictions to observed FeLV outbreak

To evaluate the performance of our FIV-based model, we also predicted FeLV transmission dynamics using three alternative models: random networks, home range overlap-based networks, and a well-mixed model. The random networks model used Erdős-Rényi random networks, matching network densities from the FIV-based model (Table S1), but otherwise allowing edges to occur between any pairs of individuals. Overlap-based networks were generated using the degree distributions of panther home range overlap networks from 2002-2004 and simulated annealing with the R package *statnet* ([49]; supplementary methods). For both random and overlap-based networks, FeLV transmission was simulated as in the FIV-based simulations. The well-mixed model was a stochastic, continuous time compartmental model (Gillespie algorithm), with rate functions aligning with the chain binomial FeLV transmission probabilities (see supplementary methods).

We performed transmission simulations for all *model types* (FIV-based, overlap-based, random, and well-mixed) across a range of reasonable parameter space (Table S1), using a Latin hypercube design (LHS) to generate 150 parameter sets that efficiently sampled parameter space [50,51]. For each parameter set and model type, we performed 50 simulations (30,000 total). In each simulation, we recorded the number of mortalities and the duration of

278 outbreaks, which were each summarized (medians) across each parameter set. For each model
279 type, we determined if each parameter set's predicted median mortalities, duration of outbreaks,
280 and abortive cases were within a reasonable range based on the observed FeLV outbreak (5-20
281 mortalities, 78-117 week duration, at least 5 abortive infections; [29]). If so, a parameter set was
282 deemed "feasible" for that model type. Ranges were used to account for uncertainty in
283 observations and population size in this cryptic species (supplementary methods). To test for
284 differences in the frequency of feasible FeLV predictions between model types, we fit a binomial
285 generalized linear mixed model (GLMM), assuming a logistic regression with "feasible" (vs
286 "unfeasible") as the outcome, model type as a predictor variable, and a random intercept for
287 parameter set.

288 We tested for spatial clustering of cases in the observed FeLV outbreak by leveraging
289 our database of qPCR-based FeLV status. We performed a local spatial clustering analysis of
290 FeLV cases and controls using SaTScan (50% maximum, circular window; [52]). A SaTScan
291 analysis seeks to identify clusters of cases in which the observed cases within a particular
292 cluster exceed random expectation; this analysis reports the observed/expected ratio and radius
293 of any significant clusters. In addition, we performed a global cluster analysis with Cuzick and
294 Edward's test (global cluster detection with case-control data) in the R package *smacpod* (1, 3,
295 5, 7, 9, and 11 nearest neighbors; 999 iterations; [53–55]). To determine if simulated FeLV
296 cases likewise demonstrated spatial clustering, we repeated SaTScan local cluster analysis and
297 Cuzick and Edward's tests (at 3, 5, and 7 nearest neighbors) with feasible FIV-based simulation
298 results. To determine if detected clustering in FIV-based simulations was simply based on our
299 respawning protocol, we also performed both spatial analyses with feasible overlap-based
300 simulation results as a "negative control." Because the overlap-based model was not spatially
301 explicit, we assigned the same geographic locations to nodes in the overlap-based networks
302 from the corresponding FIV-based networks.

To determine if certain transmission parameters were important for feasible outcomes, we performed post hoc random forest variable importance analyses for each of the four model types with “feasible” as the binary response variable (using the R package randomForest [56,57]; see supplementary results).

Results

FIV transmission network analysis

In the main FIV network, Phyloscanner inferred 42 potential transmission relationships (edges) between 19 individuals (nodes; network density = 0.25), after removing 9 edges that were between individuals known not to be alive at the same time (Figure 3). Panther FIV genomes missing from the transmission network were those for whom transmission relationships could not be inferred by Phyloscanner (see Discussion). ERGM results for the main FIV network identified triangle (*gwesp*) and star structures (*altkstar*) as key structural variables, and age category and log transformed pairwise geographic distance as key transmission variables (Tables 1, S2). Though altkstar was not statistically significant, inclusion of this variable contributed to improved AIC and goodness of fit outcomes. Adults were more likely to be involved in transmission events (but see discussion of sample size limitations) and inferred transmission events were more likely between individuals which were geographically closer to each other. The fitted model showed reasonable goodness of fit (Figures S2-3).

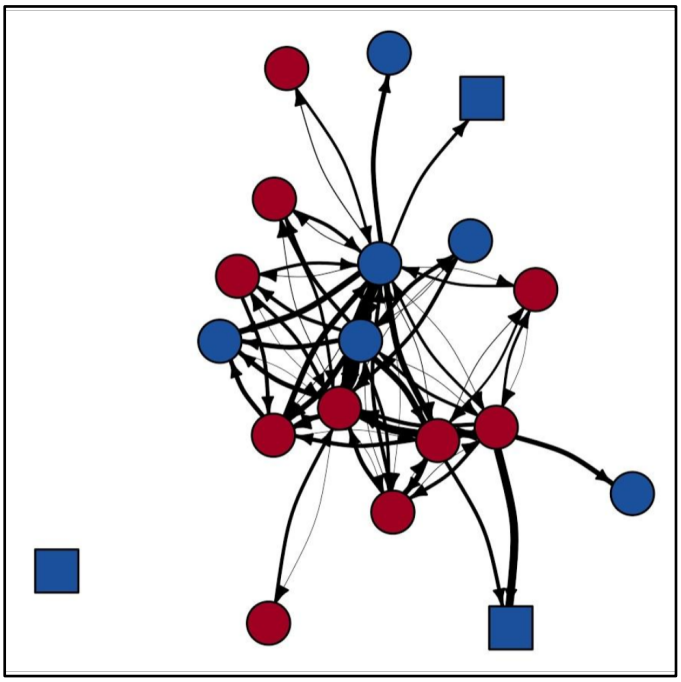

Figure 3: *Phyloscanner-derived main FIV transmission network. Node shape indicates panther age class (square = subadult; circle = adult). Node color indicates panther sex (blue = male; red = female). Edge weight represents Phyloscanner tree support for each edge (thicker edge = increased support); for visualization purposes, edges are displayed as the inverse of the absolute value of the log of these support values. While pictured as a directed and weighted network, statistical analyses used binary, undirected networks.*

Table 1: Main FIV transmission network exponential random graph model results

Variable	**Estimate**	**SE**	***p*-value**
Edges (intercept)	-2.56	1.33	0.055
gwesp	0.98	0.26	<0.001
altkstar	-0.70	0.96	0.47
Age (Adult)	0.93	0.44	0.03
Log pairwise distance	-0.45	0.21	0.03

Note: "gwesp" is geometrically weighted edgewise shared partner distribution (a representation of triangle structures) and "altkstar" is alternating k-stars (a representation of star structures). Age classes were subadult and adult, with subadults the reference level; pairwise distances were between home range centroids and log-transformed. Only those variables from the final model are shown. Estimates shown are untransformed; SE represents standard error; p-*values less than 0.05 were considered statistically significant.*

FeLV simulations

About 9% of parameter sets across all model types were classified as feasible (Figures S6-S7). The FIV-based model had the highest odds of feasibility, though this difference did not achieve statistical significance (Table 2). SaTScan analysis of observed FeLV status found weak evidence of local spatial clustering (two clusters detected, but not statistically significant with p=0.165 and 0.997, respectively; Figure S5). Cuzick and Edward's tests found evidence of global clustering at 3, 5, and 7 nearest neighbor levels (test statistic T_k where k is number of nearest neighbors considered: $T_3 = 20$, $p = 0.049$; $T_5 = 32$, $p = 0.028$; $T_7 = 43$, $p = 0.023$). Feasible parameter sets from both the FIV-based and overlap-based models produced some evidence of local and global spatial clustering of simulated FeLV cases (Figures 4, S8). However, the FIV-based model better captured the size and strength of predicted local clusters (SaTScan radius and observed/expected cases, respectively; Figure 4) and was moderately better at capturing global spatial patterns (Figure S8).

The post-hoc random forest analyses typically showed poor balanced accuracy and area under the curve (AUC) results. However, the parameter shaping transmission from regressively infected individuals (C), consistently showed support for weak to moderate transmission from regressives (i.e., C = 0.1 or 0.5; Figure S11).

Table 2: Fixed effects results from model-type performance GLMM*

Variable	Estimate	SE	*p*-value
Intercept	0.055	0.40	<0.001
FIV-based network model	1.55	0.42	0.30
Random network model	1.32	0.43	0.52
Overlap-based network model	1.21	0.44	0.66

**Note: estimates provided are exponentiated; the well-mixed model was the reference group and none of the model-type results achieved statistical significance.*

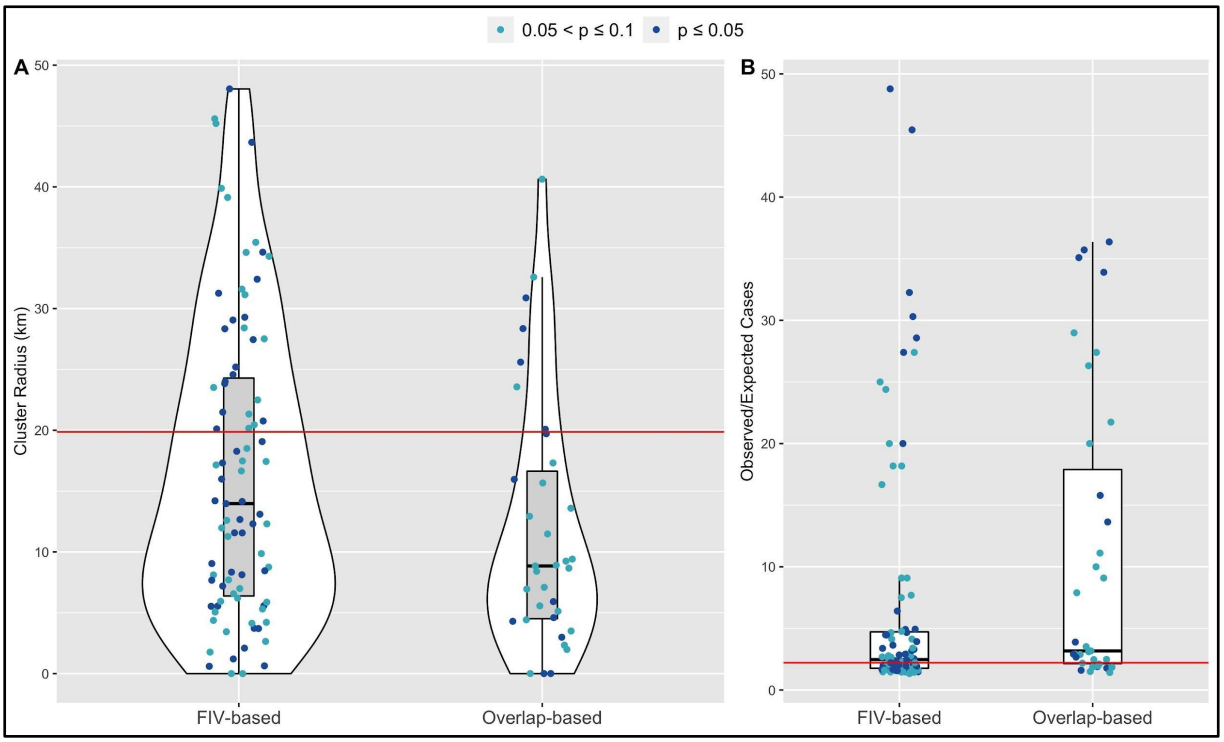

Figure 4: *SaTScan cluster analysis for feasible FIV-based and overlap-based network simulations show stronger agreement for the FIV-based model, compared to the overlap-based model, between empirical observations (red horizontal lines) and model predictions for (A) FeLV cluster size and (B) Observed/Expected FeLV cases associated with the top detected cluster. Shown are feasible simulation results in which at least one cluster was detected with* p*-values less than or equal to 0.1; further, only the results from the top cluster are shown.*

Discussion

In this study we develop a new approach whereby we leverage knowledge of transmission dynamics of a common apathogenic agent to prospectively predict dynamics of an uncommon and virulent pathogen. Our approach was distinctly different from simpler models we tested, as the apathogenic (FIV)-based approach focused on underlying drivers or mechanisms of transmission and could be used to prospectively identify predictors of transmission and develop disease control plans prior to an outbreak of a virulent pathogen (FeLV). We found that FIV transmission in panthers is primarily driven by distance between home range centroids and age class, and that our prospective FIV-based approach predicted FeLV transmission dynamics at least as well as simpler or more reactive approaches. While we do not propose that this apathogenic agent approach could accurately predict exactly when, where, and to whom transmission might occur, our results support the role of apathogenic agents as novel tools for prospectively determining sources of individual-level heterogeneity in transmission and consequently improving proactive disease management.

An FIV-based model captures FeLV transmission dynamics

We found that our network model based on drivers of FIV transmission produced FeLV outbreak predictions consistent with the observed FeLV outbreak. The FIV-based approach performed at least as well as simpler models, per our GLMM analysis, with evidence that FIV better predicted the observed spatial dynamics for FeLV transmission. A key difference between the FIV-based approach and other spatially explicit methods is that FIV allowed us to determine the importance of spatial dynamics prospectively and then translate to predictions of FeLV transmission, rather than relying on retrospective FeLV spatial analyses. Furthermore, while more complex potential drivers of transmission (e.g., host relatedness or assortative mixing by age or sex) were not found to be important for FIV transmission, these may yet be key for structuring transmission in other systems. Simpler model types like random networks or

395 metapopulation models may struggle to make transmission predictions that incorporate these
396 drivers of transmission-relevant contact. The predictive power we observed here using an
397 apathogenic virus could thus open new opportunities to determine behavioral and ecological
398 drivers of individual-level heterogeneity in the context of pathogen transmission, and even
399 shape proactive epidemic management strategies for pathogens such as FeLV.

400 Our network statistical analysis (ERGMs) determined that pairwise geographic distances
401 and age category structure FIV transmission in the Florida panther. These findings are well
402 supported by panther and FIV biology, providing confidence in the functioning of our
403 apathogenic agent workflow. For example, panthers are wide-ranging animals but maintain
404 home ranges, and this appears to translate to increased transmission between individuals that
405 are close geographically. This finding is supported by the tendency for FIV phylogenies to show
406 distinct broad [58] and fine scale [59] geographic clustering in *Puma concolor*. Further,
407 specifically among Florida panthers, spatial autocorrelation of FIV exposure status was
408 previously found to approach statistical significance [60]. The wide-ranging nature of puma
409 appears to limit geographic clustering of many infectious agents [60], with FIV a notable
410 exception to this pattern. In addition, because FIV is a persistent infection, we would expect
411 cumulative risk of transmission to increase over an individual's lifetime and adults would
412 consequently be involved in more transmission events. The low number of subadult individuals
413 in our dataset, however, means that this finding must be interpreted with some caution.

414 With these ERGM results in mind, key components of the success of our apathogenic
415 agent approach are likely that (1) FIV is a largely species-specific virus with transmission
416 pathways closely matching intraspecific transmission of FeLV, and (2) both FIV and FeLV,
417 perhaps unusually for infectious agents of puma, display spatial clustering of infection. Here,
418 FIV fundamentally acted as a proxy for close, direct contact in panthers, and could consequently
419 determine drivers of such contacts. If, for example, FIV also exhibited strong vertical or
420 environmental transmission, we would no longer expect the predictive success for FeLV we

421 observed here. This consideration highlights the importance of careful apathogenic agent
422 selection when attempting to predict pathogen transmission, a workflow which must now be
423 tested in additional host-pathogen systems. For example, the mixed results when using
424 commensal agents to identify close social relationships in other systems [15–18,21,22]
425 highlights that some host-apathogenic agent combinations will work better than others for
426 determining drivers of transmission. Within our study, Phyloscanner struggled to elucidate
427 transmission relationships between many of our FIV genomes, likely due to unusually low
428 genetic diversity among our FIV isolates, or our use of proviral DNA (which has lower diversity
429 than circulating RNA) [35]. While the drivers of transmission we identified are biologically
430 reasonable, we may have lacked the power to identify more complex relationships (e.g.,
431 homophily) due to the low number of individuals in our transmission network.

432 Elaborating on agent selection suggestions outlined in the introduction, we propose that
433 apathogenic agent selection should carefully consider agent genetic diversity within a target
434 population—not just expected diversity based on typical mutation rates, as in our case—and
435 favor those agents with high diversity to facilitate transmission inference. We also propose that
436 apathogenic agents should represent the timescales of transmission for the pathogen of
437 interest. For example, FeLV produces long, slow epidemics, such that FIV transmission
438 relationships may be most representative across the longer timescales we evaluated here. In
439 contrast, short, acute pathogen epidemics would likely best be represented by apathogenic
440 agent transmission over shorter timescales. Our results highlight that, perhaps most importantly,
441 an apathogenic agent should have a well characterized mode of transmission that closely
442 matches transmission of the pathogen of interest, as this was likely key to our success with FIV
443 and FeLV. Future research should determine how divergent an apathogenic agent may be from
444 a pathogen of interest while still predicting transmission dynamics.

445 While few parameter sets in our simulations were classified as feasible, this appears to
446 be predominantly the result of the wide range of parameter space explored through our LHS

447 sampling design. This limitation was fundamentally due to uncertainties in FeLV transmission
448 parameters, and is representative of the uncertainties experienced in predicting transmission of
449 emerging or understudied pathogens. Infectiousness of regressives, the number of introductions
450 of FeLV to the panther population, and the duration of FeLV infection in panthers were all
451 important sources of uncertainty in our models. All three of these dynamics can have significant
452 impacts on the duration of a simulated epidemic, allowing an epidemic to continue to "stutter"
453 along at low levels [61], much as was observed in the empirical FeLV outbreak. Our *post hoc*
454 random forest analysis provided some evidence of weak transmission from regressive
455 individuals, but this finding would need to be validated with additional research, as it is in stark
456 contrast to FeLV dynamics in domestic cats. Reducing uncertainties in these three key
457 dynamics would significantly narrow the range of our predictions, and even assist in ongoing
458 management efforts for FeLV in endangered panthers. The effect of transmission parameter
459 uncertainties underscores the importance of linking laboratory and model-based research to
460 generate more accurate transmission forecasts [62].
461
462 *Limitations and future directions*
463 The suite of tools for inferring transmission networks from infectious agent genomes is
464 rapidly expanding [24]. In this study, we used the program Phyloscanner as it maximized the
465 information from our deep sequencing viral data. However, our FIV sequences were generated
466 within a tiled amplicon framework [35,63], which biases intrahost diversity and limits viral
467 haplotypes [64]. Phyloscanner was originally designed to analyze RNA from virions and not
468 proviral DNA, as we have done here. We have attempted to mitigate the effects of these
469 limitations by analyzing several different Phyloscanner outputs to confirm consistency in our
470 results, and by using only binary networks to avoid putting undue emphasis on transmission
471 network edge probabilities, as these are likely uncertain. Further, our primary conclusions from
472 the transmission networks—that age and pairwise distance are important for transmission—are

biologically plausible and supported by other literature, as discussed above. Nevertheless, future work should evaluate additional or alternative transmission network inference platforms.

In addition, ERGMs assume the presence of the “full network” and it is as yet unclear how missing data may affect transmission inferences [38]. ERGMs are also prone to degeneracy with increased complexity and do not easily capture uncertainty in transmission events, as most weighted network ERGM (or generalized ERGM) approaches have been tailored for count data (e.g., [65]). ERGMs may therefore not be the ideal solution for identifying drivers of transmission networks in all systems. Alternatives may include advancing dyad-based modeling strategies [66], which may more easily manage weighted networks and instances of missing data.

Our FIV-based approach required extensive field sampling, and many disciplines from viral genomics through simulation modeling. However, with increasing availability of virome data and even field-based sequencing technology, our approach may become more accessible with time. Further, the predictive benefits seen here, while needing further testing and validation, could become a key strategy for proactive pathogen management in species of conservation concern, populations of high economic value (e.g. production animals), populations with infrequent pathogen outbreaks that make targeted surveillance more difficult, or populations at high risk of spillover, all of which may most benefit from rapid, efficient epidemic responses.

Conclusions

Here, we integrated genomic and network approaches to identify drivers of FIV transmission in the Florida panther. This apathogenic agent acted as a marker of close, direct contact transmission, and was subsequently successful in predicting the observed transmission dynamics of the related pathogen, FeLV. Further testing of apathogenic agents as markers of transmission and their ability to predict transmission of related pathogens is needed, but holds promise for revolutionizing proactive epidemic management across host-pathogen systems.

Acknowledgements

Thanks to M. Michalska-Smith, K. Worsley-Tonks, J. Mistrick, and S. N. Hart for key feedback. This research was supported by the National Science Foundation (DEB-1413925, 1654609, and 2030509). MLJG was supported by the Office of the Director, National Institutes of Health (NIH T32OD010993), the University of Minnesota Informatics Institute MnDRIVE program, and the Van Sloun Foundation. JLM was supported by the ACVP/STP Coalition for Veterinary Pathology Fellows and the Linda Munson Fellowship for Wildlife Pathology Research. The content is solely the responsibility of the authors and does not necessarily represent the official views of the National Institutes of Health. Puma icon by Freepik at Flaticon.com.

Data Availability

Data and R code for replication of simulations and analyses is available on GitHub (https://github.com/mjones029/FIV_FeLV_Transmission) and upon acceptance will be archived at Zenodo.

Works Cited

1. Anderson RM, May RM. 1991 *Infectious Diseases of Humans: Dynamics and Control*. OUP Oxford.
2. Metcalf CJE, Lessler J. 2017 Opportunities and challenges in modeling emerging infectious diseases. *Science* **357**, 149–152.
3. Drewe JA. 2010 Who infects whom? Social networks and tuberculosis transmission in wild meerkats. *Proc. Biol. Sci.* **277**, 633–642.
4. Morris M, Kretzschmar M. 1995 Concurrent partnerships and transmission dynamics in networks. *Soc. Networks* **17**, 299–318.
5. Cauchemez S, Bhattarai A, Marchbanks TL, Fagan RP, Ostroff S, Ferguson NM, Swerdlow D, Pennsylvania H1N1 working group. 2011 Role of social networks in shaping disease transmission during a community outbreak of 2009 H1N1 pandemic influenza. *Proc. Natl. Acad. Sci. U. S. A.* **108**, 2825–2830.

528 6. Craft ME, Caillaud D. 2011 Network models: an underutilized tool in wildlife epidemiology?
529 *Interdiscip. Perspect. Infect. Dis.* **2011**, 676949.

530 7. Keeling MJ, Eames KTD. 2005 Networks and epidemic models. *J. R. Soc. Interface* **2**, 295–
531 307.

532 8. Keeling MJ, Woolhouse MEJ, May RM, Davies G, Grenfell BT. 2003 Modelling vaccination
533 strategies against foot-and-mouth disease. *Nature* **421**, 136–142.

534 9. Lloyd-Smith JO, George D, Pepin KM, Pitzer VE, Pulliam JRC, Dobson AP, Hudson PJ,
535 Grenfell BT. 2009 Epidemic dynamics at the human-animal interface. *Science* **326**, 1362–
536 1367.

537 10. Dobson AP *et al.* 2020 Ecology and economics for pandemic prevention. *Science* **369**,
538 379–381.

539 11. Knight-Jones TJD, Rushton J. 2013 The economic impacts of foot and mouth disease--
540 What are they, how big are they and where do they occur? *Prev. Vet. Med.* **112**, 161–173.

541 12. Williams ES, Thorne ET, Appel MJ, Belitsky DW. 1988 Canine distemper in black-footed
542 ferrets (*Mustela nigripes*) from Wyoming. *J. Wildl. Dis.* **24**, 385–398.

543 13. Roelke-Parker ME *et al.* 1996 A canine distemper virus epidemic in Serengeti lions
544 (*Panthera leo*). *Nature* **379**, 441–445.

545 14. Sillero-Zubiri C, King AA, Macdonald DW. 1996 Rabies and mortality in Ethiopian wolves
546 (*Canis simensis*). *J. Wildl. Dis.* **32**, 80–86.

547 15. Bull CM, Godfrey SS, Gordon DM. 2012 Social networks and the spread of Salmonella in a
548 sleepy lizard population. *Mol. Ecol.* **21**, 4386–4392.

549 16. Blasse A, Calvignac-Spencer S, Merkel K, Goffe AS, Boesch C, Mundry R, Leendertz FH.
550 2013 Mother-offspring transmission and age-dependent accumulation of simian foamy virus
551 in wild chimpanzees. *J. Virol.* **87**, 5193–5204.

552 17. Chiyo PI, Grieneisen LE, Wittemyer G, Moss CJ, Lee PC, Douglas-Hamilton I, Archie EA.
553 2014 The influence of social structure, habitat, and host traits on the transmission of
554 *Escherichia coli* in wild elephants. *PLoS One* **9**, e93408.

555 18. Blyton MDJ, Banks SC, Peakall R, Gordon DM. 2013 High temporal variability in
556 commensal *Escherichia coli* strain communities of a herbivorous marsupial. *Environ.*
557 *Microbiol.* **15**, 2162–2172.

558 19. Lax S *et al.* 2014 Longitudinal analysis of microbial interaction between humans and the
559 indoor environment. *Science* **345**, 1048–1052.

560 20. Song SJ *et al.* 2013 Cohabiting family members share microbiota with one another and with
561 their dogs. *Elife* **2**, e00458.

562 21. VanderWaal KL, Atwill ER, Isbell LA, McCowan B. 2014 Linking social and pathogen
563 transmission networks using microbial genetics in giraffe (*Giraffa camelopardalis*). *J. Anim.*
564 *Ecol.* **83**, 406–414.

565 22. Springer A, Mellmann A, Fichtel C, Kappeler PM. 2016 Social structure and Escherichia coli
566 sharing in a group-living wild primate, Verreaux's sifaka. *BMC Ecol.* **16**, 6.

567 23. Archie EA, Tung J. 2015 Social behavior and the microbiome. *Current Opinion in*
568 *Behavioral Sciences* **6**, 28–34.

569 24. Hall MD, Woolhouse MEJ, Rambaut A. 2016 Using genomics data to reconstruct
570 transmission trees during disease outbreaks. *Rev. Sci. Tech.* **35**, 287–296.

571 25. Gilbertson MLJ, Fountain-Jones NM, Craft ME. 2018 Incorporating genomic methods into
572 contact networks to reveal new insights into animal behaviour and infectious disease
573 dynamics. *Behaviour* **155**, 759–791.

574 26. Blyton MDJ, Banks SC, Peakall R, Lindenmayer DB, Gordon DM. 2014 Not all types of host
575 contacts are equal when it comes to E. coli transmission. *Ecol. Lett.* **17**, 970–978.

576 27. Archie EA, Luikart G, Ezenwa VO. 2009 Infecting epidemiology with genetics: a new
577 frontier in disease ecology. *Trends Ecol. Evol.* **24**, 21–30.

578 28. Carver S *et al.* 2016 Pathogen exposure varies widely among sympatric populations of wild
579 and domestic felids across the United States. *Ecol. Appl.* **26**, 367–381.

580 29. Cunningham MW *et al.* 2008 Epizootiology and management of feline leukemia virus in the
581 Florida puma. *J. Wildl. Dis.* **44**, 537–552.

582 30. Krakoff E, Gagne RB, VandeWoude S, Carver S. 2019 Variation in Intra-individual Lentiviral
583 Evolution Rates: a Systematic Review of Human, Nonhuman Primate, and Felid Species. *J.*
584 *Virol.* **93**. (doi:10.1128/JVI.00538-19)

585 31. Brown MA, Cunningham MW, Roca AL, Troyer JL, Johnson WE, O'Brien SJ. 2008 Genetic
586 characterization of feline leukemia virus from Florida panthers. *Emerg. Infect. Dis.* **14**, 252–
587 259.

588 32. Greene CE. 2012 *Infectious diseases of the dog and cat*. 4th ed.. St. Louis, Mo.:
589 Elsevier/Saunders.

590 33. Hartmann K. 2012 Clinical aspects of feline retroviruses: a review. *Viruses* **4**, 2684–2710.

591 34. Van De Kerk M, Onorato DP, Hostetler JA, Bolker BM, Oli MK. 2019 Dynamics,
592 persistence, and genetic management of the endangered florida panther population.
593 *Wildlife Monogr.* **203**, 3–35.

594 35. Malmberg JL *et al.* 2019 Altered lentiviral infection dynamics follow genetic rescue of the
595 Florida panther. *Proc. Biol. Sci.* **286**, 20191689.

596 36. McClintock BT, Onorato DP, Martin J. 2015 Endangered Florida panther population size
597 determined from public reports of motor vehicle collision mortalities. *J. Appl. Ecol.* **52**, 893–
598 901.

599 37. Wymant C *et al.* 2018 PHYLOSCANNER: Inferring Transmission from Within- and
600 Between-Host Pathogen Genetic Diversity. *Mol. Biol. Evol.* **35**, 719–733.

601 38. Silk MJ, Fisher DN. 2017 Understanding animal social structure: exponential random graph

models in animal behaviour research. *Anim. Behav.* **132**, 137–146.

39. Morris M, Handcock MS, Hunter DR. 2008 Specification of Exponential-Family Random Graph Models: Terms and Computational Aspects. *J. Stat. Softw.* **24**, 1548–7660.

40. Esri. USA Urban Areas (FeatureServer). See https://services.arcgis.com/P3ePLMYs2RVChkJx/arcgis/rest/services/USA_Urban_Areas/FeatureServer.

41. Fieberg J, Kochanny CO, Lanham. 2005 Quantifying home-range overlap: the importance of the utilization distribution. *J. Wildl. Manage.* **69**, 1346–1359.

42. Calenge C. 2006 The package adehabitat for the R software: tool for the analysis of space and habitat use by animals. *Ecological Modelling*. **197**, 1035.

43. Hunter DR, Handcock MS, Butts CT, Goodreau SM, Morris M. 2008 ergm: A Package to Fit, Simulate and Diagnose Exponential-Family Models for Networks. *J. Stat. Softw.* **24**, nihpa54860.

44. R Core Team. 2018 R: A Language and Environment for Statistical Computing.

45. Logan KA, Sweanor LL. 2001 *Desert Puma: Evolutionary Ecology And Conservation Of An Enduring Carnivore*. Island Press.

46. Johnson WE *et al.* 2010 Genetic restoration of the Florida panther. *Science* **329**, 1641–1645.

47. Elbroch LM, Quigley H. 2016 Social interactions in a solitary carnivore. *Curr. Zool.* **63**, 357–362.

48. Hofmann-Lehmann R, Hartmann K. 2020 Feline leukaemia virus infection: A practical approach to diagnosis. *J. Feline Med. Surg.* **22**, 831–846.

49. Handcock MS, Hunter DR, Butts CT, Goodreau SM, Morris M. 2008 statnet: Software tools for the representation, visualization, analysis and simulation of network data. *J. Stat. Softw.* **24**, 1548.

50. Marino S, Hogue IB, Ray CJ, Kirschner DE. 2008 A methodology for performing global uncertainty and sensitivity analysis in systems biology. *J. Theor. Biol.* **254**, 178–196.

51. Carnell R. 2012 lhs: Latin hypercube samples. *R package version 0.10, URL http://CRAN.R-project.org/package=lhs*

52. Kulldorff M. 1997 A spatial scan statistic. *Communications in Statistics - Theory and Methods* **26**, 1481–1496.

53. Cuzick J, Edwards R. 1990 Spatial clustering for inhomogeneous populations. *J. R. Stat. Soc.* **52**, 73–96.

54. French J. 2020 smacpod: Statistical Methods for the Analysis of Case-Control Point Data.

55. Kanankege KST, Alvarez J, Zhang L, Perez AM. 2020 An Introductory Framework for Choosing Spatiotemporal Analytical Tools in Population-Level Eco-Epidemiological

638 Research. *Front Vet Sci* **7**, 339.

639 56. Liaw A, Wiener M. 2002 Classification and Regression by randomForest. *R News*. **2**, 18–
640 22.

641 57. White LA, VandeWoude S, Craft ME. 2020 A mechanistic, stigmergy model of territory
642 formation in solitary animals: Territorial behavior can dampen disease prevalence but
643 increase persistence. *PLoS Comput. Biol.* **16**, e1007457.

644 58. Lee JS *et al.* 2014 Evolution of puma lentivirus in bobcats (*Lynx rufus*) and mountain lions
645 (*Puma concolor*) in North America. *J. Virol.* **88**, 7727–7737.

646 59. Fountain-Jones NM *et al.* 2021 Host relatedness and landscape connectivity shape
647 pathogen spread in the puma, a large secretive carnivore. *Commun Biol* **4**, 12.

648 60. Gilbertson MLJ, Carver S, VandeWoude S, Crooks KR, Lappin MR, Craft ME. 2016 Is
649 pathogen exposure spatially autocorrelated? Patterns of pathogens in puma (*Puma*
650 *concolor*) and bobcat (*Lynx rufus*). *Ecosphere* **7**, e01558.

651 61. Blumberg S, Lloyd-Smith JO. 2013 Inference of R(0) and transmission heterogeneity from
652 the size distribution of stuttering chains. *PLoS Comput. Biol.* **9**, e1002993.

653 62. Plowright RK, Sokolow SH, Gorman ME, Daszak P, Foley JE. 2008 Causal inference in
654 disease ecology: investigating ecological drivers of disease emergence. *Front. Ecol.*
655 *Environ.* **6**, 420–429.

656 63. Quick J *et al.* 2017 Multiplex PCR method for MinION and Illumina sequencing of Zika and
657 other virus genomes directly from clinical samples. *Nat. Protoc.* **12**, 1261–1276.

658 64. Grubaugh ND *et al.* 2019 An amplicon-based sequencing framework for accurately
659 measuring intrahost virus diversity using PrimalSeq and iVar. *Genome Biol.* **20**, 8.

660 65. Krivitsky PN. 2012 Exponential-family random graph models for valued networks. *Electron.*
661 *J. Stat.* **6**, 1100–1128.

662 66. Yang A *et al.* 2021 Effects of social structure and management on risk of disease
663 establishment in wild pigs. *J. Anim. Ecol.* **90**, 820-833. (doi:10.1111/1365-2656.13412)

664